JOURNAL OF COMPUTATIONAL PHYSICS 77, 221–239 (1988)

Onset of Chaos in Differential Delay Equations

JACK K. HALE* AND NATALIA STERNBERG†

Lefschetz Center for Dynamical Systems,
Division of Applied Mathematics, Brown University,
Providence, Rhode Island 02912

Received February 13, 1987; revised July 24, 1987

In the present paper we study the onset of chaos in the differential delay equation $\dot{x}(t) = -x(t) + bx(t-2)/(1+x^{10}(t-2))$, $b > 0$. We develop a new numerical technique and apply it to study the global behavior of the flow on the attractor. Using this technique, we find unstable periodic orbits, connections between different periodic orbits, transverse homoclinic orbits, and try to explain the underlying reason for chaos. © 1988 Academic Press, Inc.

INTRODUCTION

In this paper we study the onset of chaos in differential delay equations. We develop a new numerical technique and apply it to obtain results of theoretical interest.

As a model we consider the following equation:

$$\dot{x}(t) = ax(t) + b\frac{x(t-\tau)}{1+x^n(t-\tau)},$$

where n is an integer, $a < 0$, and b, $\tau > 0$. This equation describes different periodic diseases and was studied numerically by L. Glass and M. C. Mackey [5, 6], U. an der Heiden and M. C. Mackey [12], and J. D. Farmer [2].

In the first three of these papers the authors fixed three of the four parameters and integrated the equation numerically. As they were changing the fourth parameter, they observed Hopf bifurcation to a stable periodic orbit, a series of period doubling bifurcations, and chaotic behavior of the solutions. J. D. Farmer's work [2] was different. He tried to understand more about the attractor by computing its embedding dimension and found that during a chaotic regime, the embedding dimension of the attractor is at least equal to four. His computations also indicated that the system has a strange attractor. However, none of the existing numerical computations has led to an explanation of what is the underlying reason

* This research was supported in part by the Air Force Office of Scientific Research under Contract AFOSR-84-0376.

† This research was supported in part by DARPA under Contract 85F123600.

0021-9991/88 $3.00

for chaos, why the embedding dimension of the attractor is at least four, or what the behavior of the flow is for different values of the parameter. Our goal in this paper is to come closer to an answer to all of these questions.

It has been known since the time of Poincaré that a chaotic regime is associated with certain types of homoclinic orbits of a hyperbolic periodic orbit. This phenomenon was formalized by S. Smale [23], L. P. Sil'nikov [22], N. K. Gavrilov and L. P. Sil'nikov [3], S. Newhouse and J. Palis [20], S. Newhouse [18]. But at present it is not known why such chaos occurs even for ordinary differential equations. Many authors think that the onset of chaos and the appearence of strange attractors is due to the creation of a homoclinic tangency, that is, the creation of a tangency between the stable and unstable manifolds of a hyperbolic periodic orbit [19].

Let us recall that a homoclinic orbit to a hyperbolic periodic orbit is any orbit (except the periodic orbit) that belongs to both the stable and unstable manifold of the periodic orbit. The homoclinic orbit is transversal if the tangent spaces of the stable and unstable manifolds of the Poincaré map at each point of intersection span the space. The existence of a transverse homoclinic orbit always implies the existence of chaos in the sense of T. Y. Li and J. A. Yorke [17] (see, for example, [9]).

Throughout this paper, we think of the given delay equation as defining a flow on the space $C = C([-\tau, 0], R)$ of continuous real valued functions on $[-\tau, 0]$. For any function $\varphi \in C$ there is a unique solution $x(t, \varphi)$ of the given equation defined for $t \geqslant -\tau$ such that $x(t, \varphi) = \varphi(t)$ for all $t \in [-\tau, 0]$. The flow $\varphi \mapsto \Psi(t)\varphi$ is defined by $(\Psi(t)\varphi)(\theta) = x(t+\theta, \varphi)$, $\theta \in [-\tau, 0]$. With this notation periodic orbits become closed curves in C, and in this space one can define the above concepts of stable and unstable manifolds of a periodic orbit, the Poincaré map, hyperbolicity, and homoclinic orbits.

Homoclinic tangencies and transverse homoclinic orbits for scalar delay equations have been constructed in specific cases by H.-O. Walther [25], U. an der Heiden and H.-O. Walther [14], U. an der Heiden and M. C. Mackey [13], J. K. Hale and X.-B. Lin [11]. These examples show that homoclinic orbits do occur in delay equations. In [10], J. K. Hale and X.-B. Lin proved that if there is a homoclinic orbit for a general retarded fuctional differential equation, then there is an arbitrarily small perturbation of the vector field such that the perturbed equation has a transverse homoclinic orbit. We now ask if there is a homoclinic orbit for the system that we shall consider and are there connections between different periodic orbits.

In our model we choose $a = -1$, $n = 10$, $\tau = 2$, and b as a parameter.

The local analysis we give in Section 1 shows that for $b \approx 1.34$ a Hopf bifurcation to a stable T-periodic orbit does take place. From the computations done by U. an der Heiden and M. C. Mackey [12] we know that this periodic orbit becomes unstable due to a period doubling bifurcation. The computations of U. an der Heiden and M. C. Mackey [12] as well as the ones in [5, 6, 2] proceed in the following manner: starting with a given initial function, integrate the

equation and observe the stable limiting solutions. The way in which the initial function is chosen plays no essential role. However, if one is careful in the specification of the initial function, more information can be obtained about the behavior of the flow. In the study of a dynamical system, the global behavior of the flow is determined by the unstable sets, not by the stable ones. If we could know the exact behavior of the unstable manifold of the T-periodic orbit, we would be able to understand the global behavior of at least some solutions of the given dynamical system. Therefore, we must find a numerical scheme that will enable us to follow the unstable manifold of the T-periodic orbit.

The idea is simple: integrate the equation starting with the initial data sufficiently close to the unstable T-periodic orbit. Since the unstable manifold is a stable set, we obtain a good approximation of the typical flow on it (see [9] and Lambda–Lemma in [26]). There is, however, a major difficulty. How can we find the initial data for an unstable periodic orbit, which being unstable, cannot be approximated by integrating the equation? In fact, we need completely different methods from these used in [12, 5, 6, 2].

We have been able to find the initial data by tracing the bifurcation branch that corresponds to the T-periodic orbit, using the homotopy continuation method. This method has been used before by E. L. Allgower and C.-S. Chien [1], H. B. Keller [16], K. Georg [4], and others to study bifurcation diagrams of elliptic equations, and of a specific delay equation. Similar ideas were used by E. Doedel [27] in the case of parabolic partial differential equations. As an integration technique we use the spectral method that was introduced by K. Ito and R. Teglas [15] primarily for linear delay equations. Although our equation is nonlinear, this method continues to provide sufficiently good accuracy. A detailed description of our numerical scheme is given in Section 3.

The main advantage of our algorithm is that it makes it possible to find unstable peiodic orbits, heteroclinic and homoclinic orbits, and to follow certain solutions which until now could not be observed numerically. It also provides a better understanding of the flow on the attractor. Using our scheme to study the dynamics of the given system for different values of the parameter, we obtain a number of results that are described in detail in Section 2. The following is an outline of those results.

For $b \approx 1.56$ we observe the first period doubling bifurcation to a stable $2T$-periodic orbit. There is a connection between the T-periodic and $2T$-periodic orbits.

For $b \approx 1.72$ the $2T$-periodic orbit becomes unstable and a $4T$-periodic orbit appears. There are connections between the orbits of period T and $2T$, the orbits of period T and $4T$, and the orbits of period $2T$ and $4T$.

For $1.725 \leqslant b \leqslant 1.74$ several period doubling bifurcations occur. As a result, we observe new periodic orbits of period $8T$, $16T$, and $32T$.

Furthermore, there is a parameter value b_0, $1.74 < b_0 < 1.77$ such that for $b = b_0$ there is a homoclinic tangency between the stable and the unstable manifolds of the T-periodic orbit.

For $b = 1.77$ there is a transverse homoclinic orbit.

We suspect that the creation of a homoclinic tangency occurs in the following way. The period of some stable periodic orbit continues to increase and, as b approaches b_0, some point on this orbit approaches the T-periodic orbit, giving the homoclinic tangency.

In order to understand more about the attractor, one must study the changes in the characteristic multipliers of the T-periodic orbit. It turns out that for $b < 1.8$ the unstable manifold of the Poincaré map for the T-periodic orbit is one dimensional. For $b \approx 1.8$ a saddle-node bifurcation from the T-periodic orbit takes place and the unstable manifold becomes two-dimensional. The dominant multiplier inside the unit circle is real, but for $b \approx 1.93$ it becomes complex. In all of these cases, the transverse homoclinic orbit still exists. This suggests that one would need a four-dimensional analog of the Hénon map to model the Poincaré map for the flow on the attractor, which coincides with J. D. Farmer's result on the embedding dimension of the attractor.

Further study is obviously required here, but that would go beyond the goals of the present paper.

As mentioned before, the creation of some homoclinic orbits leads to the creation of a horseshoe map, to infinitely many periodic orbits, and to the onset of chaos. We suspect that our system behaves in a similar way. It is quite possible that a two-dimensional unstable manifold leads to the creation of more homoclinic orbits. In addition, a complex dominant characteristic multiplier inside the unit circle could also lead to the creation of generalized Sil'nikov [21] type orbits. All this could cause chaotic behavior of the flow.

1. Local Analysis

Consider the differential delay equation

$$\dot{x}(t) = -x(t) + b\frac{x(t-2)}{1+x^{10}(t-2)}, \tag{1}$$

where $b > 0$ is a parameter.

Proposition. (a) *If $b < 1$, then $x_0 = 0$ is the unique equilibrium solution of the given equation, and it is stable.*

(b) *A pitchfork bifurcation from the trivial equilibrium solution x_0 takes place at $b = 1$, and x_0 becomes unstable.*

(c) *If $b > 1$, then the given equation has three equilibrium solutions: $x_0 = 0$, $x_1 = (b-1)^{1/10}$ and $x_2 = -x_1$. Moreover, there exists a parameter value $b = b_0 > \frac{10}{9}$ such that x_1 and x_2 are stable for all $1 < b < b_0$.*

(d) *There is a Hopf bifurcation from x_1 to a positive periodic orbit, and from x_2 to a negative periodic orbit at $b = b_0$.*

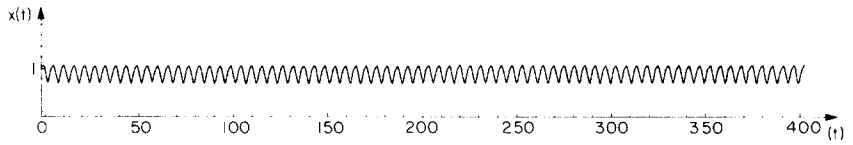

FIG. 1. The stable T-periodic orbit at $b = 1.516$; $T \approx 5.5$.

Remark. Numerical computations, done in Section 3, show that the Hopf bifurcation from x_1 occurs at the parameter value $b_0 \approx 1.34$. As a result, a stable positive periodic orbit of period $T \approx 5.5$ appears (see Fig. 1).

We first prove the following lemma.

LEMMA. *Consider the equation*

$$z = -1 + de^{-2z} \tag{2}$$

over the field of complex numbers, where $d \neq 0$ is a parameter:

(a) *If $0 < d < 1$, then all solutions z of* (2) *have negative real parts.*

(b) *There exists a value $d_0 < 0$ such that Eq.* (2) *has a pure imaginary solution at $d = d_0$.*

Proof of the Lemma. (a) Let $0 < d < 1$ be arbitrary, but fixed. Let $z = \mu + iv$. Using Eq (2), we obtain for μ and v the system of equations

$$\begin{aligned} \mu &= -1 + de^{-2\mu}\cos(2v) \\ v &= -de^{-2\mu}\sin(2v). \end{aligned} \tag{3}$$

Assume there exists a solution (μ_0, v_0) of the system (3) such that $\mu_0 > 0$. Let $h(\mu) = de^{-2\mu}$. Since h is a strictly monotone decreasing function of μ and since $h(0) = d < 1$, it follows that $h(\mu_0) < 1$. Therefore,

$$\mu_0 = -1 + de^{-2\mu_0}\cos(2v_0) < 0.$$

This contradicts the assumption.

(b) Suppose Eq. (2) has a pure imaginary solution $z = iv_0$, $v_0 \in R$, for some parameter value $d = d_0$. This leads to the system of equations

$$\begin{aligned} 0 &= -1 + d_0\cos(2v_0) \\ v_0 &= -d_0\sin(2v_0), \end{aligned} \tag{4}$$

or, equivalently,

$$v_0 = -\tan(2v_0). \tag{5}$$

If v_0 is a positive solution of Eq. (5), then

$$-\frac{\pi}{4}+\frac{\pi}{2}n<v_0<\frac{\pi}{2}n, \qquad n=1, 2, 3, \ldots .$$

A solution v_0 of (5) can be chosen so that $d_0=1/\cos(2v_0)<0$. The pair (d_0, v_0) then satisfies the system (4). Therefore $z=iv_0$ is a solution of (2). This completes the proof of the lemma.

Proof of the Proposition. (a) Let $b<1$. All the equilibrium solutions of the given equation are obtained by solving the equation for x

$$-x+b\frac{x}{1+x^{10}}=0. \tag{6}$$

Therefore, $x=0$ is the unique equilibrium solution of (1).

In order to study the stability of the trivial solution, we have to consider the solutions of the characteristic equation about $x=0$:

$$\lambda=-1+be^{-2\lambda}. \tag{7}$$

Part (a) of the lemma implies that all solutions of Eq. (7) have negative real parts, and therefore, x_0 is stable (see [8]).

(b) The characteristic equation about $x=0$ is given by (7). Obviously, $\lambda=0$ is a solution of (7) for $b=1$. For $b>1$, it follows from (6) that the given equation (1) has three equilibrium solutions, namely, $x_0=0$, $x_1=(b-1)^{1/10}$, and $x_2=-x_1$. Hence, for $b=1$, a pitchfork bifurcation takes place. Moreover, the implicit function theorem implies that for any parameter value $b>1$ but close to 1, Eq. (7) has a real-valued solution λ.

Suppose all real-valued solutions λ of (7) are negative for $b>1$. Let $h(\lambda)=be^{-2\lambda}$. Since h is a strictly monotone decreasing function of λ and since $h(0)=b>1$, it follows that $h(\lambda)>1$. Therefore,

$$\lambda=-1+be^{-2\lambda}>0.$$

This contradicts the assumption. So, $\lambda>0$ and the trivial solution is unstable.

(c) In part (b) we showed that Eq. (1) has three equilibrium solutions x_0, x_1, and x_2 for $b>1$. The characteristic equation about x_1 is

$$\lambda=-1+Be^{-2\lambda}, \tag{8}$$

where $B=(10-9b)/b$. Since $b>1$, it follows that $B<1$.

If $1<b<10/9$, we have $0<B<1$, and part (a) of the lemma implies that $\mathrm{Re}(\lambda)<0$ for all solutions λ of (8).

If $b=\frac{10}{9}$, then $B=0$, and it follows that $\lambda=-1$ is a solution of (8).

Furthermore, part (b) of the lemma implies that there is a parameter value $B_0<0$

such that $\mathrm{Re}(\lambda)=0$ at $B=B_0$. This means there is a parameter value $b_0>\frac{10}{9}$ such that $\mathrm{Re}(\lambda)=0$ at $b=b_0$. Since $\mathrm{Re}(\lambda)$ is a continuous function of b and since $\mathrm{Re}(\lambda)\neq 0$ for all $b\in(1, b_0)$, we obtain that $\mathrm{Re}(\lambda)<0$ for all $b\in(1, b_0)$. This implies that the equilibrium solution x_1 of the given equation (1) is stable. Since x_1 and x_2 have the same characteristic equation, x_2 is also stable.

(d) We already know that for $b=b_0$ Eq. (8) has a solution $\lambda_0=\mu_0+iv_0$, where $\mu_0=0$, and $v_0\in R$.

The second condition for the occurence of a Hopf bifurcation is (see [8])

$$\left.\frac{d\,\mathrm{Re}(\lambda)}{db}\right|_{b=b_0}>0.$$

We now show that this condition is also satisfied.

Let $\mu=\mathrm{Re}(\lambda)$ and $v=\mathrm{Im}(\lambda)$. It is easy to see, using (3) at $d=B$, that

$$\frac{d\mu}{db}=-\frac{10}{b^2}e^{-2\mu}\cos(2v)-2Be^{-2\mu}\cos(2v)\frac{d\mu}{db}-2Be^{-2\mu}\sin(2v)\frac{dv}{db},$$

and

$$\frac{dv}{db}=\frac{10}{b^2}e^{-2\mu}\sin(2v)+2Be^{-2\mu}\sin(2v)\frac{d\mu}{db}-2Be^{-2\mu}\cos(2v)\frac{dv}{db}.$$

Using (4) at $d_0=B_0$, we obtain

$$\begin{aligned}\frac{d\mu(\mu_0, v_0, b_0)}{db}&=-\frac{10}{b_0^2}\cos(2v_0)-2B_0\cos(2v_0)\frac{d\mu(\mu_0, v_0, b_0)}{db}\\&\quad-2B_0\sin(2v_0)\frac{dv(\mu_0, v_0, b_0)}{db}\\&=-\frac{10}{B_0b_0^2}-2\frac{d\mu(\mu_0, v_0, b_0)}{db}+2v\frac{dv(\mu_0, v_0, b_0)}{db},\end{aligned}$$

and

$$\begin{aligned}\frac{dv(\mu_0, v_0, b_0)}{db}&=\frac{10}{b_0^2}\sin(2v_0)+2B_0\sin(2v_0)\frac{d\mu(\mu_0, v_0, b_0)}{db}-2B_0\cos(2v_0)\frac{dv(\mu_0, v_0, b_0)}{db}\\&=-\frac{10v_0}{B_0b_0^2}-2v_0\frac{d\mu(\mu_0, v_0, b_0)}{db}-2\frac{dv(\mu_0, v_0, b_0)}{db}.\end{aligned}$$

This implies that

$$(9+4v_0^2)\frac{d\mu(\mu_0, v_0, b_0)}{db}=-\frac{10}{B_0b_0^2}(3+2v_0^2).$$

Since $B_0 < 0$, it follows that

$$\frac{d\mu(\mu_0, \nu_0, b_0)}{db} > 0.$$

By uniqueness, we see that the new periodic solution must remain positive for all time. Since the positive and the negative equilibrium solutions have the same characteristic equations, this completes the proof of the proposition.

2. Global Behavior of the Flow as Suggested by Numerical Computations

In order to understand the global behavior of solutions of the given differential delay equation, we have to analyze different periodic orbits, establish connections between them, find homoclinic orbits, and understand the structure of the attractor. Because of the symmetry property of the given equation, the corresponding positive and negative solutions behave in a similar way. Throughout the rest of this paper we will study the behavior of the flow only near the positive periodic solutions. The first step is to compute the characteristic multipliers of the stable T-periodic orbit for different values of the parameter b (see Table I). We obtain the following results.

For the stable T-periodic orbit the two dominant multipliers of the Poincaré map are real; one is negative, the other is positive. As b increases, the negative multiplier decreases and the positive one increases.

At $b \approx 1.56$ the negative multiplier becomes less than -1. This indicates that a period doubling bifurcation has taken place. As a result, the T-periodic orbit becomes unstable and a stable $2T$-periodic orbit appears. The unstable manifold of the Poincaré map for the T-periodic orbit is one-dimensional. The dominant multiplier inside the unit circle is real and increases as b increases.

In order to find the connection between the two orbits, we follow the unstable manifold of the T-periodic orbit. An approximation of the flow on the unstable manifold of the T-periodic orbit for $b \approx 1.61$ is shown on Fig. 2. We see that the unstable manifold leaves the neighborhood of the T-periodic solution and approaches the $2T$-periodic solution. This suggests that the flow for the Poincaré map behaves as shown in Fig. 3.

In Fig. 4 we can see the changes in the shape of the $2T$-periodic orbit as b changes, but the global behavior of the flow remains the same.

For $b \approx 1.72$ the approximated unstable manifold of the T-periodic orbit approaches a $4T$-periodic solution (see Fig. 5). This suggests that a period doubling bifurcation from the $2T$-periodic orbit to a stable $4T$-periodic orbit has taken place and that the $2T$-periodic orbit has become unstable. Since the $4T$-periodic orbit is stable, the ω-limit set of points on the unstable manifold of the $2T$-periodic orbit must be the $4T$-periodic orbit. Thus, there is a connection between the $2T$- and $4T$-periodic orbits. Before the bifurcation to the $4T$-periodic orbit occured, the unstable manifold of the T-periodic orbit and the stable manifold of the $2T$-periodic orbit

TABLE I

Characteristic Multipliers

b	Real part	Imaginary part
$0.151699982043810D+01$	$-0.756035161203480D+00$	$0.000000000000000D+00$
	$0.449698539623050D-02$	$-0.658396338957620D-02$
	$0.281299409888840D+00$	$0.000000000000000D+00$
	$0.181078080176250D-02$	$0.000000000000000D+00$
$0.155794551702760D+01$	$-0.990824386938670D+00$	$0.000000000000000D+00$
	$0.155295816559260D-02$	$-0.615607076669970D-02$
	$0.392158750482490D+00$	$0.000000000000000D+00$
	$0.249074208507170D-02$	$0.000000000000000D+00$
$0.156084281196150D+01$	$-0.102143389111490D+01$	$0.000000000000000D+00$
	$0.710936720349230D-03$	$-0.504423365129350D-02$
	$0.414970187980770D+00$	$0.000000000000000D+00$
	$0.253096959480210D-02$	$0.000000000000000D+00$
$0.158687959079500D+01$	$-0.116180114029520D+01$	$0.000000000000000D+00$
	$-0.140168731753380D-02$	$-0.320989539773120D-02$
	$0.509945925304210D+00$	$0.000000000000000D+00$
	$0.333143679269030D-02$	$0.000000000000000D+00$
$0.161075160290380D+01$	$-0.125481775331190D+01$	$0.000000000000000D+00$
	$-0.224071971295490D-02$	$-0.279039444082870D-02$
	$0.570166970232390D+00$	$0.000000000000000D+00$
	$0.415446123980250D-02$	$0.000000000000000D+00$
$0.168680777240210D+01$	$-0.149031721967810D+01$	$0.000000000000000D+00$
	$-0.446384617662420D-02$	$-0.174441252970240D-02$
	$0.762890215215050D+00$	$0.000000000000000D+00$
	$0.856189623248260D-02$	$0.000000000000000D+00$
$0.172000178674920D+01$	$-0.156481096680890D+01$	$0.000000000000000D+00$
	$-0.511389011543220D-02$	$-0.291165424223650D-02$
	$0.844912542767850D+00$	$0.000000000000000D+00$
	$0.128670830548570D-01$	$0.000000000000000D+00$
$0.177850494837940D+01$	$-0.165315658096530D+01$	$0.000000000000000D+00$
	$-0.571829890503110D-02$	$-0.533196150264910D-02$
	$0.966393782247140D+00$	$0.000000000000000D+00$
	$-0.249233199111000D-01$	$0.000000000000000D+00$
$0.179956246717590D+01$	$-0.167202767672700D+01$	$0.000000000000000D+00$
	$-0.573206576990730D-02$	$-0.613994509680250D-02$
	$0.100228066091180D+01$	$0.000000000000000D+00$
	$-0.169841420036980D-01$	$0.000000000000000D+00$
$0.182011239778790D+01$	$-0.168301976903950D+01$	$0.000000000000000D+00$
	$-0.557475229591050D-02$	$-0.688352008845750D-02$
	$0.103336646684970D+01$	$0.000000000000000D+00$
	$-0.115392916717700D-01$	$0.000000000000000D+00$
$0.184158556735260D+01$	$-0.168723155112470D+01$	$0.000000000000000D+00$
	$-0.501899837051820D-02$	$-0.773643704446960D-02$
	$0.107113657696480D+01$	$0.000000000000000D+00$
	$-0.655535662680050D-02$	$0.000000000000000D+00$
$0.193405102928140D+01$	$-0.167372844737020D+01$	$0.000000000000000D+00$
	$-0.392675722389150D-02$	$-0.836404675663720D-02$
	$0.109858390009020D+01$	$0.000000000000000D+00$
	$-0.261885433633490D-02$	$0.000000000000000D+00$

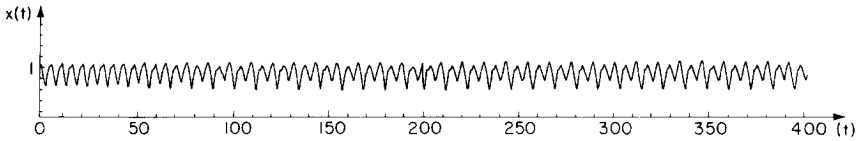

FIG. 2. The solution on the unstable manifold of the T-periodic orbit approaching the $2T$-periodic orbit at $b = 1.61$.

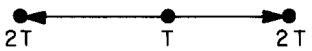

FIG. 3. The flow on the unstable manifold of the Poincaré map at $b = 1.61$.

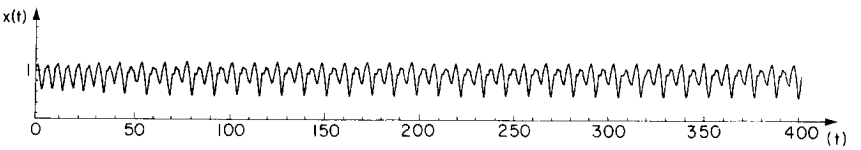

FIG. 4. The solution on the unstable manifold of the T-periodic orbit approaching the $2T$-periodic orbit at $b = 1.68$.

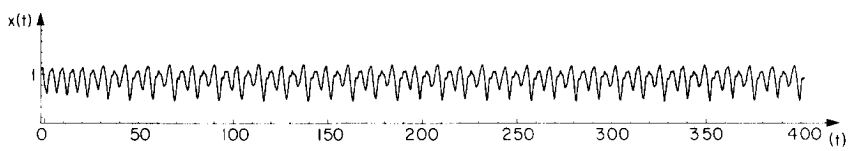

FIG. 5. The solution on the unstable manifold of the T-periodic orbit approaching the $4T$-periodic orbit at $b = 1.72$.

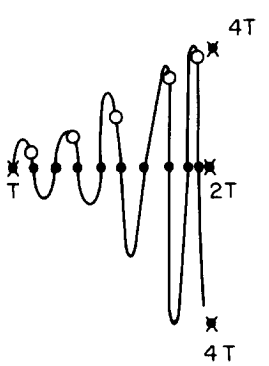

FIG. 6. The flow on the unstable manifold of the Poincaré map at $b = 1.72$: ◦ a typical orbit on the unstable manifold approaching the $4T$-periodic orbit; • the connection of the T-periodic orbit to the $2T$-periodic orbit.

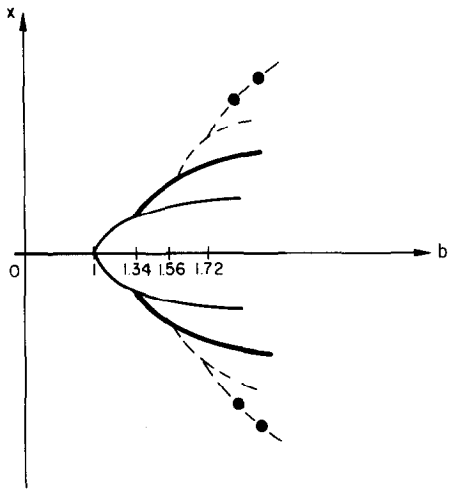

FIG. 7. The bifurcation diagram for $0 < b < 1.72$ in the space $C \times R$: ——— the equilibrium solution; ——— the T-periodic solution; - - - the $2T$-periodic solution; – • – the $4T$-periodic solution.

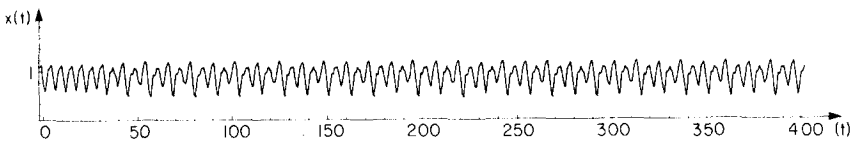

FIG. 8. The solution on the unstable manifold of the T-periodic orbit approaching the $8T$-periodic orbit at $b = 1.725$.

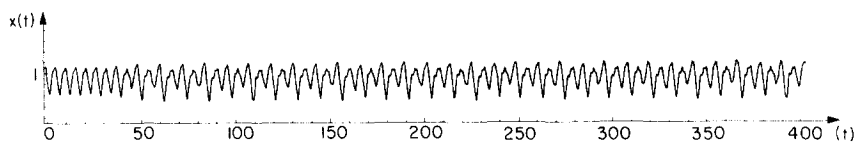

FIG. 9. The solution on the unstable manifold of the T-periodic orbit approaching the $16T$-periodic orbit at $b = 1.735$.

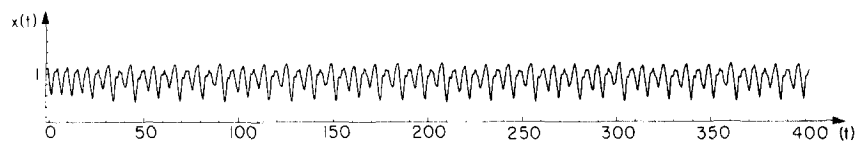

FIG. 10. The solution on the unstable manifold of the T-periodic orbit approaching the $32T$-periodic orbit at $b = 1.74$.

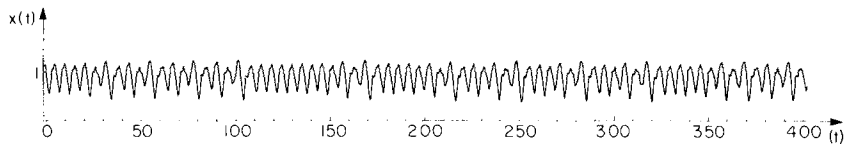

FIG. 11. The transverse homoclinic orbit at $b = 1.77$ for $0 \leqslant t \leqslant 400$.

were transversal. They should therefore remain transversal after the bifurcation takes place. This shows that there is a connection between the T- and $2T$-periodic orbits. It also implies that there is a connection between the T- and $4T$-periodic orbits. In fact, almost all initial data close to the T-periodic orbit should approach the $4T$-periodic orbit; that is, numerically, one should not observe the connection between the T- and $2T$-periodic orbits. This is confirmed in Fig. 5. The flow for the Poincaré map is indicated in Fig. 6.

The behavior of the characteristic multipliers for the T-periodic orbit did not change. The two dominant multipliers are real. One is outside the unit circle, negative, and decreases as b increases getting farther away from -1. The other is inside the unit circle, positive, and increases as b increases getting closer to 1.

So far we have the bifurcation diagram as shown in Fig. 7.

For $1.725 \leqslant b \leqslant 1.74$ several period doubling bifurcations occur (see Figs. 8–10).

For $b \approx 1.77$ (see Figs. 11, 11a) we notice that the computed solution, which approximates the unstable manifold, leaves the neighborhood of the T-periodic solution, but after a while it returns into the neighborhood of the T-periodic solution. This picture keeps repeating itself, which indicates that there is a transversal intersection of the stable and unstable manifold of the T-periodic orbit. The transversality was checked by observing numerically that the same phenomenon occurs when the initial data is perturbed. From Figs. 11, 11a, it follows that there must be some value of the parameter $1.74 < b_0 < 1.77$ for which there is a homoclinic tangency.

It is very difficult to give an explanation of what happens in the parameter range 1.74 to 1.77. Up to the parameter value $b = 1.74$ we observe several period doubling bifurcations, and we also know that a homoclinic tangency must occur at some b_0, $1.74 < b_0 < 1.77$. From the general theory of the creation of homoclinic tangencies, it is known (see, for example, [3]) that there always can be a sequence of period doublings as well as transient chaos for some values of b as b approaches b_0 from below. The orbits that come from the general theory, however, are always unstable.

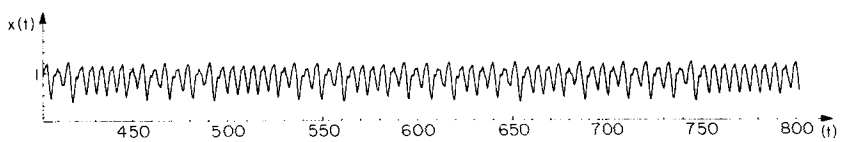

FIG. 11a. The transverse homoclinic orbit at $b = 1.77$ for $400 \leqslant t < 800$.

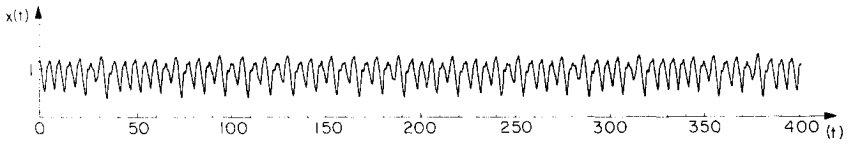

FIG. 12. The transverse homoclinic orbit at $b = 1.8$.

On the other hand, it is possible that there are still some stable periodic orbits whose periods become very large, and as b approaches b_0, some points of those approach the T-periodic orbit. A closer inpsection of Fig. 10 suggests that this is the case. In fact, one observes a distinctive peak at $t = 20$, 103, 160, 220 which is reproduced and is approximately equal to the T-periodic orbit. If this speculation is correct, then the creation of the homoclinic tangency is clear. The period of some stable periodic orbit continues to increase and, as b approaches b_0, some point on this orbit approaches the T-periodic orbit. This implies the existence of a homoclinic orbit to the T-periodic orbit at $b = b_0$.

Two other interesting phenomena happen as b increases. For $b \approx 1.80$ the dominant characteristic multiplier of the T-periodic orbit inside the unit circle becomes greater than 1. This means that a saddle-node bifurcation from the T-periodic orbit has occured. The unstable manifold of the T-periodic orbit becomes two-dimensional.

The dominant characteristic multiplier of the T-periodic orbit inside the unit circle is real, decreases as b increases, and for $b \approx 1.93$ becomes complex. In both cases the transverse homoclinic orbit still exists (see Fig. 12). This suggests that one would need a four-dimensional analog of the Hénon map to model the Poincaré map for the flow on the attractor.

It is quite possible that a two-dimensional unstable manifold leads to the creation of more homoclinic orbits. In addition, a complex dominant characteristic multiplier inside the unit circle could also lead to the creation of a Sil'nikov type orbit [21]. All of this could cause chaotic behavior of the flow.

3. FOLLOWING THE UNSTABLE MANIFOLD

In this section we present the numerical scheme for following the unstable manifold of the T-periodic orbit that has enabled us to obtain the results described in the previous section.

Main Idea and Strategy

The main idea is to integrate the equation with initial data close to the unstable T-periodic orbit. Then the computed solution will approximate the typical flow on the unstable manifold. In order to find the initial data, we use the following strategy:

(a) Choose $b^* < 1.34$, but close to this value, and the pair (x^*, b^*), where $x^* = (b^* - 1)^{1/10}$ represents a point on the bifurcation branch which corresponds to the positive equilibrium solution (see Fig. 7).

(b) Use the homotopy continuation method to follow this branch to the bifurcation point at (x, b) where $b \approx 1.34$. This is the point where Hopf bifurcation takes place.

(c) At the bifurcation point switch to the branch that corresponds to the stable T-periodic orbit (see Fig. 7).

(d) Trace this branch beyond the bifurcation point (x, b), $b \approx 1.56$, where the first period doubling bifurcation takes place. Any pair (x, b) beyond this bifurcation point represents a point on the bifurcation branch such that x is the initial data of the unstable T-periodic solution for the parameter value $b > 1.56$.

(e) In order to follow the unstable manifold of the T-periodic orbit, integrate the given equation using the initial data obtained in (d).

Integration Technique and Discretization

In order to integrate the given equation numerically, we use the spectral method which was proposed in [15] for perturbed linear systems.

Let $C = C([-2, 0], R)$ be the space of all continuos functions from $[-2, 0]$ into R. For any $\varphi \in C$ there is a unique solution $x(t)$ of the given equation defined for $t \geqslant -2$ such that $x(\theta) = \varphi(\theta)$ for all $\theta \in [-2, 0]$.

Let $z(t, \theta) = x(t + \theta)$ where x is a solution of the given equation and $\theta \in [-2, 0]$. Any smooth solution z then satisfies the boundary value problem

$$z_t = z_\theta$$

with the boundary condition

$$z_t(t, 0) = f(z(t, 0), z(t, -2)),$$

where

$$f(z(t, 0), z(t, -2)) = -z(t, 0) + b \frac{z(t, -2)}{1 + z^{10}(t, -2)}$$

and with the initial condition

$$z(0, \theta) = x(\theta), \qquad \theta \in [-2, 0].$$

If we know the solution $z(t, \theta)$ of this boundary value problem, we can find the solution $x(t)$ of the given differential delay equation using the relation

$$x(t) = z(t, 0)$$

for all $t \geqslant 0$.

In order to integrate the boundary value problem, we use the well-known spectral method (see [7, 24]) which proceeds as follows.

Choose a number of collocation points $\theta_0, ..., \theta_n$ in the interval $[-2, 0]$ and a basis $(\Phi_0, ..., \Phi_n)$ in the approximation space B such that the matrix $(\Phi_i(\theta_j + 1))_{i,j=0,...,n}$ is nonsingular. Then, define the projection operator Π from C into B by

$$\Pi z(t, \theta) = \sum_{j=0}^{n} a_j(t)\, \Phi_j(\theta + 1),$$

where $a_j(t) \in R$ are solutions of the system of linear equations

$$\Pi z(t, \theta_i) = z(t, \theta_i)$$

for all $i = 0, ..., n$, and all $t \geqslant 0$.

In order to find the solution $z(t, \theta)$, it is sufficient to determine the coefficients $a_j(t)$ in the series expansion.

As an approximation basis let us choose the Legendre polynomials, and as collocation points let us choose $(\theta_0, ..., \theta_n)$ such that $\theta_0 + 1, ..., \theta_n + 1$ are the zeros of the Legendre polynomial of order $n + 1$. With this notation, we have

$$z(t, \theta_i) = \sum_{j=0}^{n} a_j(t)\, p_j(\theta_i + 1)$$

for all $0 \leqslant i \leqslant n$ where p_j is the Legendre polynomial of order j.

Moreover, the following equations hold

$$z_t(t, \theta_i) = \sum_{j=0}^{n} a_j'(t)\, p_j(\theta_i + 1)$$

and the well-known identities for Legendre polynomials [7] imply that

$$z_\theta(t, \theta_i) = \sum_{j=0}^{n-1} b_j(t)\, p_j(\theta_i + 1),$$

where

$$b_j(t) = (2j + 1) \sum_{k = j+1,\, j+k \text{ odd}}^{n} a_k(t).$$

Furthermore, since $p_j(1) = 1$ and $p_j(-1) = (-1)^j$, it follows that

$$z(t, 0) = \sum_{j=0}^{n} a_j(t)\, p_j(1) = \sum_{j=0}^{n} a_j(t),$$

and

$$z(t, -2) = \sum_{j=0}^{n} a_j(t)\, p_j(-1) = \sum_{j=0}^{n} (-1)^j a_j(t).$$

Substituting all of these equations into the boundary value problem, we find that

$$a_j'(t) = b_j(t), \qquad 0 \leqslant j \leqslant n-1,$$

$$z_t(t, 0) = \sum_{j=0}^{n} a_j'(t) = a_n'(t) + \sum_{j=0}^{n-1} b_j(t)$$

$$= f\left(\sum_{j=0}^{n} a_j(t), \sum_{j=0}^{n} (-1)^j a_j(t) \right),$$

and

$$z(0, \theta_i) = \sum_{j=0}^{n} a_j(0)\, p_j(\theta_i + 1) = x(\theta_i)$$

for all $0 \leqslant i \leqslant n$.

In other words, we have to solve the system of ordinary differential equations

$$a_j'(t) = b_j(t), \qquad 0 \leqslant j \leqslant n-1,$$

$$a_n'(t) = \sum_{j=0}^{n-1} b_j(t) + f\left(\sum_{j=0}^{n} a_j(t), \sum_{j=0}^{n} (-1)^j a_j(t) \right)$$

with the initial condition $a(0) = (a_0(0), ..., a_n(0))$ such that

$$a(0) = \Phi^{-1} x,$$

where

$$\Phi = \begin{pmatrix} p_0(\theta_0 + 1) & \cdots & p_n(\theta_0 + 1) \\ \vdots & \ddots & \vdots \\ p_0(\theta_n + 1) & \cdots & p_n(\theta_n + 1) \end{pmatrix}$$

and $x = (x(\theta_1), ..., x(\theta_n))$.

Choosing a Homotopy Map

Our goal now is to find the initial data of unstable periodic orbits for diffrent values of the parameter. We know that $x_b(t)$ is a T-periodic solution of the given differential delay equation for a fixed arbitrary parameter b if and only if its initial data $x_b(\theta)$, $\theta \in [-2, 0]$, is a fixed point of the Poincaré map $P: \Omega \to C$, defined by $(Px)(\theta) = x(\theta + T)$, $\theta \in [-2, 0]$, where Ω denotes the domain of P.

As it was observed in [12], the period T remains almost constant as b varies as

long as the T-periodic orbit is stable. Since we use the collocation approximation for the integration of the given equation and since the collocation points are not uniformly distributed in the interval $[-2, 0]$, small changes in the period should not affect our computations. Hence we assume that the period T remains the same for all values of the parameter b. The assumption that the T-periodic solution has a period very insensitive to b is confirmed by the numerical computations given below. With this assumption, it follows that for any pair $(x_b(\theta), b) \in \Omega \times R$, $x_b(\theta)$ is the initial data of the T-periodic orbit for the parameter value b if and only if $(x_b(\theta), b)$ is a zero of the map $H: \Omega \times R \to C$, defined by $H = \mathrm{id}\,|_\Omega - P$.

In order to find the initial data of the T-periodic solution for different values of the parameter b, we therefore must solve the equation

$$H(x, b) = 0, \tag{9}$$

where $x \in \Omega$ and $b \geqslant 0$. This can be done by using the homotopy continuation method. For a basic description of this method and further references see [1, 16, 4]. The set of all the zeros of the homotopy map H is the branch of the bifurcation diagram in the space $C \times R$ that corresponds to the T-periodic solution (see Fig. 7) and since the homotopy continuation methods enables us to follow different bifurcation branches beyond the bifurcation point, we will obtain initial data for the T-periodic orbit even after it becomes unstable.

In order to detect the period doubling bifurcation, we have to compute the characteristic multipliers of the T-periodic orbit, i.e., the spectrum of the Jacobian of the Poincaré map, since this type of bifurcation cannot be observed otherwise. Indeed, a study of how the characteristic multipliers change in response to changes in the parameter is itself an interesting question.

The homotopy continuation method can be used only if we approximate Eq. (9) by a finite dimensional problem. This can be done because P is a compact operator [8] and so we can use the collocation approximation described above. Moreover, the spectrum of P is discrete and 0 is its only accumulation point.

In order to use the scheme that we have described, it remains only to find the value of the period T. We know that for $b_0 \approx 1.34$ a Hopf bifurcation from the fixed point $x \approx 1$ occurs. Choose $b > b_0$ but close to b_0, and choose the initial condition $x(\theta_0) = \cdots = x(\theta_n) = 1$. Since the periodic orbit is stable, we approximate it simply by integrating the given delay equation numerically. Analysis of the resulting data has shown us that $T \approx 5.5$.

Discussion

The numerical method that we have described has enabled us to study the qualitative behavior of solutions of the given differential delay equation. It has allowed us to follow the unstable manifold of a periodic solution, which is the key to an understanding of the behavior of the flow on the attractor. The method makes it possibile to establish connections between different solutions and to find homoclinic orbits.

Although the spectral method was introduced in [15] primarily for perturbed linear delay equations, we found it to be an accurate scheme for a nonlinear equation. We also have checked the accuracy in the cases $n = 32$ and $n = 7$.

The algorithm has performed well even though we knew only an approximate value for the period of the T-periodic orbit. Small changes in the period T did not affect our computations.

In Fig. 1, one can see that the vector obtained by using our scheme is indeed the initial condition of the stable T-periodic orbit. This further illustrates the good performance of the algorithm.

The algorithm can also be used to find other branches of the bifurcation diagram for the given delay equation and to study the behavior near other periodic solutions. Choosing initial data in the proposed way not only increases the accuracy of the computations, it also enables us to follow certain solutions on the attractor which previously could not be observed numerically. It is this last ability that is the main advantage of the numerical scheme that we have described.

REFERENCES

1. E. L. ALLGOWER AND C.-S. CHIEN, *SISSC*, in press.
2. J. D. FARMER, *Phys. D* **4**, 366, (1982)
3. N. K. GAVRILOV, AND L. P. SIL'NIKOV, I, *Mat. Sb. USSR* **17**, 467 (1972); II, **19**, 139 (1973).
4. K. GEORG, *SIAM J. Sci. Statist. Comput.* **2**, No. 1, 35 (1981).
5. L. GLASS AND M. C. MACKEY, *Science* **197**, 287 (1977).
6. L. GLASS AND M. C. MACKEY, "Pathological Conditions Resulting from Instabilities in Physiological Control Systems," in *Bifurcation Theory and Applications*, edited by Gurel and Rossler (N. Y. Acad. Sci., New York, 1979), p. 214.
7. D. GOTTLIEB AND A. ORSZAG, *Numerical Analysis of Spectral Methods: Theory and Applications* (SIAM, Philadelphia, 1977).
8. J. K. HALE, *Theory of Functional Differential Equations* (Springer-Verlag, New York/Berlin, 1977).
9. J. K. HALE AND X.-B. LIN, *Ann. Mat. Pura Appl.* (IV) **144**, 229 (1986).
10. J. K. HALE AND X.-B. LIN, *J. Differential Equations* **65**, 175 (1986).
11. J. K. HALE AND X.-B. LIN, *Nonlinear Anal.* **10**, 693 (1986).
12. U. AN DER HEIDEN, AND M. C. MACKEY, *Funct. Biol. Med.* **1**, 156 (1982).
13. U. AN DER HEIDEN AND M. C. MACKEY, *J. Math. Biol.* **16**, 75 (1982).
14. U. AN DER HEIDEN AND H.-O. WALTHER, *J. Differential Equations* **47**, 2, 273 (1983).
15. K. ITO, R. TEGLAS, *SIAM J. Control Optim.* **24**, 737, (1986).
16. H. B. KELLER, "Numerical solution of bifurcation and nonlinear eigenvalue problems," in *Applications of Bifurcation Theory*, edited by P. H. Rabinowitz (Academic Press, New York, 1977), p. 348.
17. T. Y. LI AND J. A. YORKE, *Amer. Math. Monthly* **82**, 985 (1975).
18. S. NEWHOUSE, *Topology* **13**, 9 (1974).
19. S. NEWHOUSE, "Asymptotic behavior and homoclinic points in nonlinear systems," in *Nonlinear Dynamics*, edited by Helleman (N. Y. Acad. Sci., New York, 1980), p. 292.
20. S. NEWHOUSE AND J. PALIS, "Bifurcation of Morse-Smale dynamical systems," in *Dynamical Systems*, edited by Peixoto (Academic Press, New York, 1973).
21. L. P. SIL'NIKOV, *Math. Sb. USSR* **10**, 91 (1970).
22. L. P. SIL'NIKOV, *Math. Sb. USSR* **3**, 353 (1967).
23. S. SMALE, *Bull. Amer. Math. Soc.* **73**, 747 (1967).

24. N. STERNBERG, *J. Comput. Phys.* **72**, 422 (1987).
25. H.-O. WALTHER, *J. Nonlinear Anal.* **5**, 775 (1981).
26. J. PALIS AND W. DE MELO, *Geometric Theory of Dynamical Systems* (Springer-Verlag, New York, 1982).
27. E. DOEDEL, "Continuation technique in the study of chemical reaction schemes," in *Mathematical Methods in Energy Research, Laramie, Wyo.*, 1982/1983 (SIAM Summary, Philadelphia, 1984), p. 103.